

Three different routes from the directed Ising to the directed percolation class

Su-Chan Park

Institut für Theoretische Physik, Universität zu Köln, Zùlpicher Strasse 77, 50937 Köln, Germany

Hyunggyu Park

School of Physics, Korea Institute for Advanced Study, Seoul 130-722, Korea

(Dated: November 29, 2018)

Scaling nature of absorbing critical phenomena is well understood for the directed percolation (DP) and the directed Ising (DI) systems. However, a full analysis of the crossover behavior is still lacking, which is of our interest in this study. There are three different routes from the DI to the DP classes by introducing a symmetry breaking field (SB), breaking a modulo 2 conservation (CB), or making channels connecting two equivalent absorbing states (CC). Each route can be characterized by a crossover exponent, which is found numerically as $\phi = 2.1 \pm 0.1$ (SB), 4.6 ± 0.2 (CB), and 2.9 ± 0.1 (CC), respectively. The difference between the SB and CB crossover can be understood easily in the domain wall language, while the CC crossover involves an additional critical singularity in the auxiliary field density with the memory effect to identify itself independent.

PACS numbers: 64.60.Ht, 05.70.Ln, 89.75.Da

I. INTRODUCTION

Critical behavior of absorbing phase transitions can be categorized by universality classes [1]. The most well-known example is the directed percolation (DP) class which may be (loosely) defined by a classification scheme known as the “DP conjecture” [2, 3, 4]. The conjecture states that models exhibiting a continuous transition into a *single* absorbing state should belong to the DP class unless symmetry or conservation is involved. The DP conjecture is not complete in two folds. First, some models with infinitely many absorbing states such as the pair contact process [5] also belong to the DP class, at least in its stationary property, unless there is no clear-cut symmetry among absorbing states [6, 7, 8]. Second, the conjecture itself does not resolve the controversy related to the pair contact process with diffusion (PCPD) [9, 10, 11, 12, 13, 14].

However, this conjecture is useful enough to trigger a search for a non-DP universality class. One can find several universality classes in Ref. [1] which do not meet the constraint of the DP conjecture. Among them, this paper interests in the system with two equivalent absorbing states (or in general two equivalent groups of many absorbing states) [15, 16, 17, 18, 19]. The Ising-like Z_2 symmetry between two absorbing states which is sometimes manifest as a modulo 2 conservation of domain walls in one dimension renders the system to exhibit a non-DP critical behavior. This universality class has several names such as the parity conserving [15, 16], the directed Ising (DI) [17, 20, 21] which will be used to refer to this class in this paper, the generalized voter class [22] and so on. In higher dimensions, all these classes become distinct.

The Ising symmetry (or the modulo 2 conservation) *per se* is not enough to force the DI critical behavior. It requires an infinite dynamic barrier between two equivalent (group of) absorbing states [6, 20], which is analogous to

the free energy barrier between two ordered states in the equilibrium Ising model. A state near one absorbing state cannot evolve into the other absorbing state within a finite number of successive local changes. In other words, a domain wall (frustration) in a configuration generated by pasting two absorbing states cannot disappear by itself, so the system never becomes absorbing with a single frustration [6, 10].

As an example without this additional feature, consider a one-dimensional system of diffusing particles with pair annihilation ($2A \rightarrow 0$) and branching of two particles by a triplet ($3A \rightarrow 5A$). We may map this particle model onto the ferromagnetic Ising spin model by interpreting a particle as a domain wall of the Ising system as follows:

$$\begin{aligned} A\emptyset \leftrightarrow \emptyset A &\mapsto \uparrow\downarrow \leftrightarrow \uparrow\uparrow, \\ AA \rightarrow \emptyset\emptyset &\mapsto \uparrow\downarrow \rightarrow \uparrow\uparrow, \\ \emptyset AAA\emptyset \rightarrow AAAAA &\mapsto \downarrow\uparrow\downarrow\uparrow \rightarrow \downarrow\uparrow\downarrow\uparrow, \end{aligned} \quad (1)$$

where A (\emptyset) stands for a particle (vacancy) and \uparrow (\downarrow) represents a up (down) spin. Clearly the number of domain walls is conserved modulo 2 and there are two absorbing states in the spin system (all spins are up or down) which are equivalent. However, the states with only one (diffusing) particle are also absorbing in the particle model. In the spin language, these extra absorbing states can be obtained by connecting two equivalent absorbing states (for example, $\dots \uparrow\uparrow\downarrow\downarrow \dots$), which violate the infinite dynamic barrier requirement for the DI universality class mentioned above [6, 20]. It is numerically shown that this system shares the critical behavior with the DP not the DI [10, 23], while a similar system with $2A \rightarrow 0$ and $2A \rightarrow 4A$ belongs to the PCPD class [24]. It is claimed that a long-term memory plays a crucial role in differentiating these two universality classes [11].

According to the above criterion for the DI class, one can conceive three possible routes along which the

DI critical behavior crosses over to the DP in one dimension. Introducing a symmetry breaking field (SB) [20, 25, 26, 27, 28], allowing dynamics which breaks the modulo 2 conservation (CB) [29, 30], or making channels connecting two equivalent absorbing states (CC) [6, 8] drives the system into the DP class. But these three routes bring about different characteristics in the absorbing states. The SB route maintains the absorbing states but breaks the probabilistic balance between them. The CB route (for example, by adding $A \rightarrow 0$ or $2A$) invalidates the mapping between the spin and the particle model, and ends up with only one absorbing state (vacuum). The CC route is accompanied by additional (infinitely many) absorbing states connecting two equivalent absorbing states with both the symmetry and the mapping sustained.

To quantify the difference of these routes, we measure the crossover exponents governing the crossover behavior. In Sec. II, one-dimensional models are introduced belonging to the DI class. In Sec. III, numerical results for the crossover exponents along three different routes are reported. We discuss and summarize our results in Sec. IV.

II. DI MODELS

We choose two DI models for studying crossover from the DI class to the DP class: branching annihilating walks with two offspring (BAW2) [16, 19] and the interacting monomer model (IM) which is a simplified version of the interacting monomer-monomer model [8]. We study the macroscopic absorbing phase transitions [23] inherent in the model. The suitable order parameters will be defined when we explain each model in detail. For convenience, the order parameter for different models will be denoted by ρ throughout the paper. We only study one dimensional lattice systems with periodic boundary conditions.

For the simulation of the BAW2, we take the dynamic branching rule of Ref. [29]. The simulation algorithm is detailed as follows: At first, we choose a particle residing at a lattice point randomly among, say, N_t particles present at time t . It may hop to a randomly chosen nearest neighbor site with probability p . If the target site is already occupied, two particles are removed immediately. With probability $(1 - p)$, this selected particle branches two particles along one of two directions. If an offspring is created on a site already occupied, both particles annihilate immediately. After the above steps, time increases by $1/N_t$. Since the absorbing state is vacuum, the order parameter ρ is the particle density. At criticality, the density is expected to decay as $\rho(t) \sim t^{-\delta}$ with the DI critical exponent $\delta \simeq 0.285$ [19]. Figure 1 locates the critical point at $p_c = 0.51035(5)$ which is more accurate than that obtained in Ref. [29].

The IM is a lattice model with two possible states at each lattice point; either vacant or occupied by a particle.

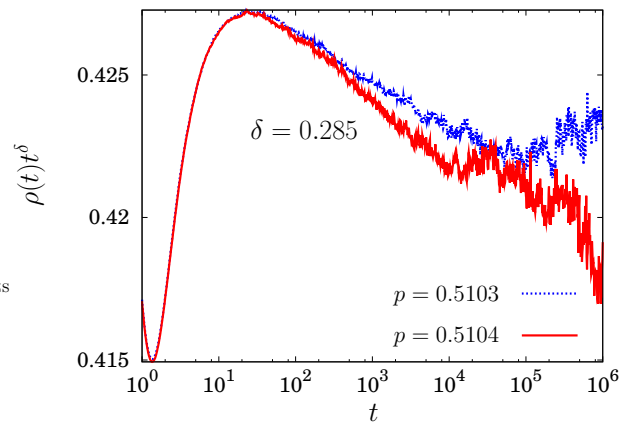
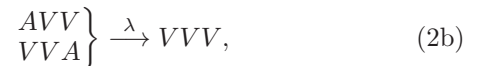


FIG. 1: (Color online) Semilogarithmic plot of $\rho(t)t^\delta$ vs t near criticality for the BAW2. The critical point is found to be $p_c = 0.51035(5)$ with the figure in the parentheses as uncertainty of the last digit.

The dynamics begins with the adsorption attempt at a randomly selected vacant site. When both of nearest neighbor (nn) sites are vacant, a monomer is adsorbed with rate 1. In case only one of the nn sites is occupied, the monomer is adsorbed on the substrate with rate λ , then reacts and leaves the substrate with the neighboring particle ($A+A \rightarrow \emptyset$) instantaneously. When both nn sites are already occupied, the adsorption attempt is rejected. The dynamics on the substrate can be summarized as



where A (V) means the monomer occupied (vacant) site.

The absorbing states of the IM are characterized by the “antiferromagnetically ordered” state ($\dots AVAVAV \dots$) and have the Z_2 symmetry (poisoning even or odd sites by monomers). Starting with initial configurations without any AA pair, the proper order parameter ρ is the density of VV pairs.

The mapping of the dynamics of the IM to that of the contact process with the modulo 2 conservation [CP(2)] [31] is possible, though there are some subtleties which make these two models a little bit different. If we assign a domain wall excitation, say X , in the middle of the VV pair, the domain wall dynamics is exactly the same as the CP(2) rules. A pair annihilation in the CP(2) corresponds to an adsorption process of a monomer as in Eq. (2a) and a pair branching in the CP(2) to an annihilation process Eq. (2b). Note that the reaction (2b) always generates two domain walls (two VV pairs), because an AA pair is not allowed in the IM. However, there is no one-to-one correspondence between configurations of the CP(2) and the IM, in general. For example, a domain wall configuration $X\emptyset X$ is not possible in the IM by definition, but possible in the CP(2) in principle. Nevertheless, if we start with the fully occupied domain

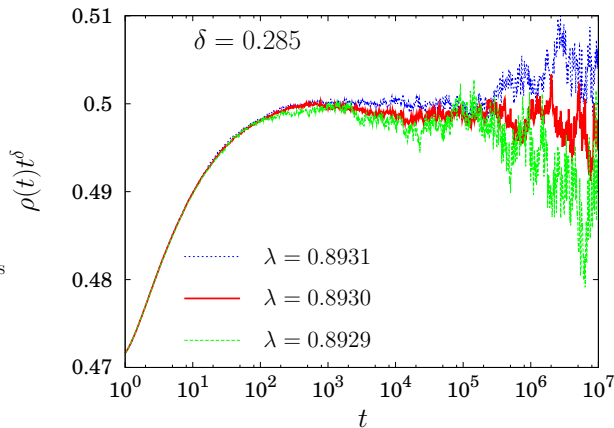


FIG. 2: (Color online) Semilogarithmic plot of $\rho(t)t^\delta$ vs t near criticality for the IM. The critical point is found to be $\lambda_c = 0.8930(1)$.

wall state, such a configuration cannot be generated by dynamics and thus the mapping becomes exact. In this case, the parameter q in Ref. [31] for the CP(2) is related to $1/(1+2\lambda)$ of the IM with suitable time rescaling. This mapping guarantees that the IM should belong to the DI class which is confirmed by Fig. 2. We found the critical point of the IM to be $\lambda_c = 0.8930(1)$ and correspondingly the more accurate critical point of the CP(2) as $q_c = 0.358\,94(3)$ than that in Ref. [31].

III. THREE ROUTES TO THE DP CLASS

To study the crossover from the DI class to the DP class, we introduce dynamics with rate w which breaks either the symmetry or the mod-2 conservation. The crossover scaling ansatz of the order parameter at criticality is [14, 32]

$$\rho(t; \Delta, w) = t^{-\delta} F(\Delta^{\nu_{\parallel}} t, w^{\mu_{\parallel}} t), \quad (3)$$

where Δ is the deviation of a tuning parameter from the DI critical point. The meaning of Δ and w will be made clearer in the context of each crossover model. When $w = 0$, the scaling function in Eq. (3) should describe the DI critical behavior. Hence, δ and ν_{\parallel} are the critical exponents of the DI classes; $\delta \simeq 0.285$ and $\nu_{\parallel} \simeq 3.2$, respectively [19]. The crossover exponent is defined as $\phi = \nu_{\parallel}/\mu_{\parallel}$ which can be measured from observing how the phase boundary behaves near the DI critical point

$$1/\phi = \lim_{w \rightarrow 0^+} \frac{\ln \Delta_c(w)}{\ln w}, \quad (4)$$

where $\Delta_c(w)$ is the distance from the DI critical point at $w = 0$ to the DP critical point at nonzero w .

First, consider the conservation-breaking (CB) route by introducing the mod-2 conservation breaking dynamics to the BAW2. When a particle tries to branch off-

spring, the number of offspring is 2 (1) with the probability $1 - w$ (w). This crossover model with finite w will be referred to as the BAWCB.

Second, the symmetry-breaking (SB) route is constructed by introducing the symmetry breaking dynamics to the IM in such a way that the adsorption rate Eq. (2a) at even-indexed sites is different from that of odd-indexed sites. To be specific, we modify adsorption dynamics without affecting the desorption events as



where the subscripts o and e refer to an odd- and even-indexed sites, respectively. When $0 < w < 1$, this system prefers the absorbing state of poisoning monomers at even-indexed sites, which breaks the Z_2 symmetry of the IM. We will refer to the model with dynamics Eqs. (2a') and (2b) as the IMSB.

Finally, the channel-connecting (CC) route can be constructed by connecting two equivalent symmetric absorbing states through infinitely many absorbing configurations [6]. In the context of the IM model, this route can be studied by allowing an adsorption without a pair reaction probabilistically:



The model with dynamics of Eqs. (2a), (2b), and (2c) will be called as the IMCC. As an adsorption attempt at a vacant site between two monomers (AVA) is still rejected, any configuration without a VV pair is absorbing and the order parameter is still the VV pair density. In contrast to the IM, the IMCC has infinitely many absorbing states characterized by the AA pair density (auxiliary field density). By pasting the two antiferromagnetically ordered absorbing states, we find either $\dots VAVAAVAV \dots$ which is already absorbing, or $\dots VAVAVVAVAV \dots$ which can evolve back to an absorbing state by adsorbing a monomer at either site of

TABLE I: Critical point values $\lambda_c(w)$ of the IMSB and IMCC and $p_c(w)$ of the BAWCB for various w 's. The numbers in the parentheses indicate the uncertainty of the last digits.

w	$\lambda_c(w; \text{IMSB})$	$\lambda_c(w; \text{IMCC})$	$p_c(w; \text{BAWCB})$
0	0.8930(1)	0.8930(1)	0.510 35(5)
10^{-5}		0.9119(1)	0.4931(1)
2×10^{-5}			0.490 30(5)
5×10^{-5}		0.92545(5)	0.4858(1)
10^{-4}		0.9340(1)	0.481 65(5)
2×10^{-4}		0.944 95(5)	0.4767(1)
3×10^{-4}			0.473 45(5)
5×10^{-4}	0.9125(2)	0.965 35(5)	0.468 90(5)
10^{-3}	0.9199(1)	0.9842(1)	0.461 75(5)
2×10^{-3}	0.9303(2)		
4×10^{-3}	0.944 75(5)		

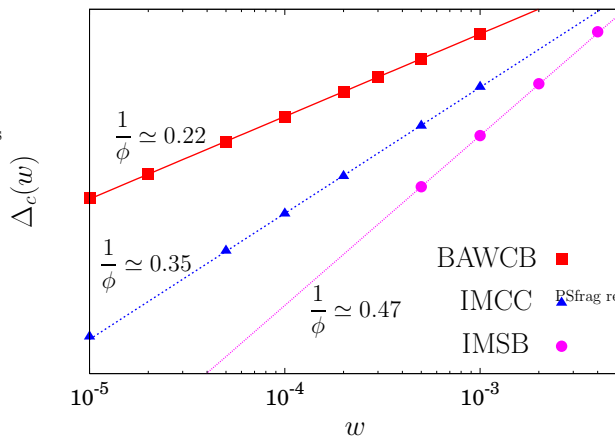


FIG. 3: (Color online) Log-log plot of $\Delta_c(w)$ vs w for three different crossover models. For graphical clarity, we shifted y axis with arbitrary scale. Each line whose slope is $1/\phi$ shows the fitting result for the corresponding phase boundary.

the VV pair. Hence there is no infinite dynamic barrier between absorbing states and the system leaves the DI class into the DP class.

Now we are equipped with three different models which can show the crossover behavior from the DI class to the DP class. As explained above, the crossover exponent ϕ can be deduced from the DP phase boundary near the DI critical point; see Eq. (4). For each model, the critical points at finite w are located numerically using the DP values of the critical exponents (see Table I). The critical points for the IMSB and IMCC are denoted by $\lambda_c(w)$ and for the BAWCB by $p_c(w)$, respectively. To measure the crossover exponent, we define $\Delta_c(w) \equiv |\lambda_c(w) - \lambda_c(0)|/\lambda_c(0)$ for the IMSB and the IMCC, and similarly $\Delta_c(w) \equiv |p_c(w) - p_c(0)|/p_c(0)$ for the BAWCB.

In Fig. 3, the crossover exponents are estimated for all three different routes. Along the SB route, we estimate $\phi = 2.1(1)$ which is consistent with previous estimates: $\phi = 2.1(1)$ [26], $2.24(10)$ [28], and recently $1.9(1)$ [33]. Along the CB route, our estimate is $\phi = 4.6(2)$ which is close to the recent result $\phi = 4.8(2)$ [33]. Along the CC route, we find $\phi = 2.9(1)$, which is clearly different from those for the SB and CB routes.

IV. DISCUSSION AND SUMMARY

The crossover behavior from one fixed point to another does not reflect the properties of both fixed points, in general. Rather, strictly speaking, it is related to one fixed point and its crossover operator which forces the system to crossover to the other fixed point [14, 32, 34]. In many cases, the crossover route is unique between two fixed points, so is the crossover operator, which leads to one unique crossover exponent between two universality classes.

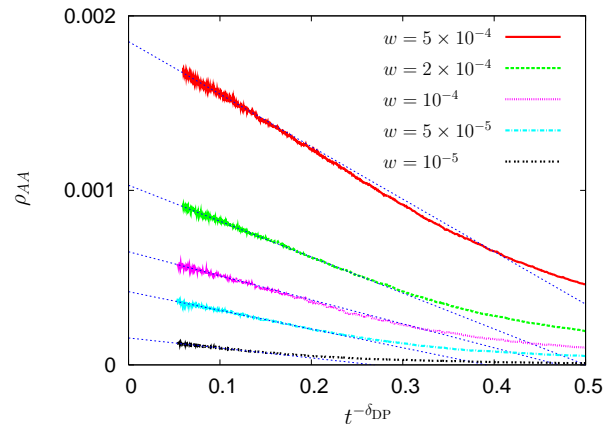


FIG. 4: (Color online) Long-time behavior of the auxiliary field density ρ_{AA} for small w 's. The exponent $\delta_{DP} \simeq 0.160$ is the temporal decay exponent of the order parameter in the DP class. Simple extrapolation lines are given by dotted lines.

However, in the case studied here, we found that there are three different routes for the crossover from the DI to the DP class, which yield all three different crossover exponents. It indicates that the crossover operator associated with each route should be different from each other. The difference between the SB and CB routes has been noticed earlier [20]. Summarizing it in the domain-wall (particle) representation, the crossover operator in the CB route is a single particle annihilation or creation operator in the action, while that in the SB route is a nonlocal string operator (global product of particle number operators) [20]. Hence it is not surprising to find that the two crossover exponents are different.

The crossover behavior along the CC route is tricky. First, note that the Z_2 symmetry between the odd-indexed and even-indexed sites is not broken in this route, which implies that the CC route is different from the SB one. Second, in terms of domain walls, the CC process, Eq. (2c), clearly breaks the mod-2 conservation in the number of VV pairs (primary field, say, X), because of which one may naively guess the CB-type crossover along the CC route. However, unlike the ordinary CB models, the CC process generates an infinite number of absorbing configurations with AA pairs (auxiliary field, say, Y) which give the feedback effect to the domain wall dynamics. Consider the dynamics of the IMCC in terms of two fields X and Y . The reactions, Eqs. (2a) and (2b), can be rewritten as $2X \rightarrow \emptyset$ and $X \rightarrow 3X$, while Eq. (2c) is equivalent to $X \rightarrow Y$. The presence of AA pairs makes it possible to allow another reaction of $XY \rightarrow 2X$ ($AVVAA \rightarrow AVVVA$) in combination with Eq. (2b). The last two reactions involving the auxiliary field represent the feedback which generates memory effects on the primary field.

The emergence of the auxiliary field density and the feedback mechanism may be responsible for the new crossover behavior along the CC route. To see how the

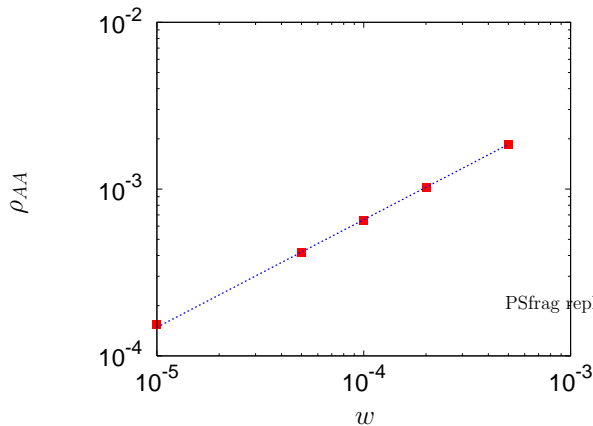


FIG. 5: (Color online) Log-log plot of ρ_{AA} in the steady state versus w . The slope of the dotted line is 0.645.

auxiliary field may affect the crossover, we measure the auxiliary field density (natural density) $\rho_{AA}(w)$ along the DP critical line. We expect its long-time temporal behavior as $\rho_{AA}(w, t) = \rho_{AA}(w) - bt^{-\delta_{DP}}$ starting from the A particle vacuum [8, 35], where δ_{DP} is the temporal decay exponent of the order parameter in the DP class. Figure 4 confirms our expectation and the asymptotic values of ρ_{AA} is plotted against w in Fig. 5. It is clear that $\rho_{AA}(0) = 0$ at the DI critical point. Near $w = 0$, the power-law singularity is found as $\rho_{AA} \sim w^\alpha$ with $\alpha = 0.65(2)$. We test the universality of the CC crossover scaling as well as the singularity of the auxiliary field density by investigating various different models like a CC variant of the interacting monomer-dimer model [36] and a two-species particle model defined as below. It turns out that these models form one crossover universality class with the same CC-type crossover exponent ϕ and the auxiliary field density exponent α [36].

To examine the exclusive role of the feedback (memory) effect, we introduce a two-species (X, Y) particle model where the feedback process can be directly controlled. The primary particles X can diffuse, while the secondary particles Y are immobile. Each species particles are hard core particles, but a simultaneous occupation by different species at a site is allowed. Therefore each site can be in one of four possible states such as \emptyset , X , Y , and XY .

The reactions dynamics is symbolically summarized as $2X \rightarrow \emptyset$, $X \rightarrow 3X$, $X \rightarrow Y$, and $XY \rightarrow Y, 2X$, or $3X$. To be more specific, the evolution rule is given as follows: First, choose one of X particles randomly. With probability w , the chosen X spontaneously mutates or annihilates as $X \rightarrow Y$ or $XY \rightarrow Y$. With probability $p - w$, the X hops to one of its neighboring sites. Whenever two X particles attempt to occupy the same site, they annihilate immediately like in the BAW2. With probability $1 - p$, the X can branch particles in the neighborhood as $X \rightarrow X + 2X$ with the dynamic branching rule [29]. To control the feedback effect, we introduce a parameter

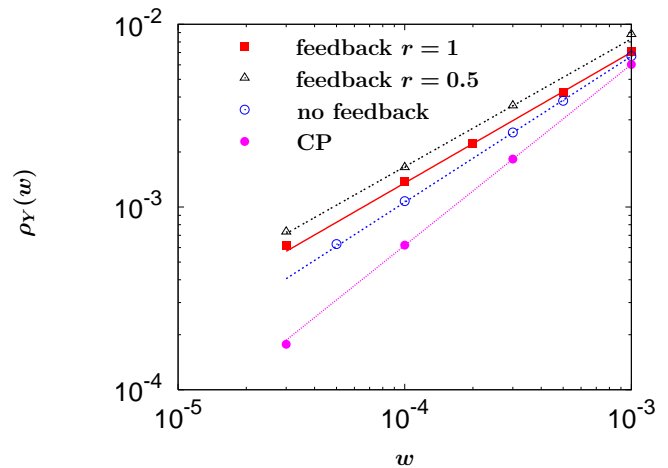


FIG. 6: (Color online) $\rho_Y(w)$ vs w along the phase boundary for the two-species model with ($r = 1$ and 0.5) or without ($r = 0$) feedback processes as well as the variant of the contact process (see text) in double logarithmic scales. The slopes of the straight lines are 0.70, 0.71, 0.80, and 1 from above.

r in the branching process when a Y resides along with the X at the same site, such that $XY \rightarrow X + 2X$ with the relative rate $(1 - r)$ and $XY \rightarrow X + X$ with r .

At $w = 0$, there is no spontaneous annihilation (or mutation) process and the model becomes exactly the same as the BAW2 after some transient period needed for removing all Y particles via branching processes. At finite w , we expect the DP scaling with a finite density of Y particles; $\rho_Y(w) > 0$ because X particles generate Y particles via mutation processes, which cannot be fully eliminated via branching processes. So the CC-type crossover is expected in general.

However the $r = 0$ point is special. There, the presence of Y particles never affects the dynamics of X particles, so there is no feedback mechanism to alter the primary particle density through the secondary particles. The primary field dynamics is basically identical to the BAWCB model introduced in Sec. III and the CB-type crossover scaling should appear at $r = 0$ along with nonzero $\rho_Y(w)$. At finite r , the X particle dynamics is affected by the presence of Y particles, which generates the memory effects on the X particle density. Hence r can be regarded as the feedback controlling parameter and w as the crossover parameter.

We performed numerical simulations for various values of r . For nonzero r , we found that the secondary particle density behaves as $\rho_Y(w) \sim w^\alpha$ with $\alpha = 0.70(3)$ and the crossover exponent $\phi = 3.1(2)$, both of which are consistent with the CC crossover results for the IMCC model within numerical errors. In contrast, at $r = 0$ the CB crossover is found as expected along with $\alpha \simeq 0.80$ different from the CC crossover case; see Fig. 6. This leads to the conclusion that the feedback process (memory) is crucial in establishing the CC-type crossover universality class and affects the singularity characteristic of the

auxiliary field density.

It is interesting to note that the numerical values of α suggest a simple conjecture that $\alpha = 1 - 1/\phi$ for the DI to the DP crossover with an emerging auxiliary field. The mean field analysis leads to $\alpha = 0$ and $\phi = 1$ (see Appendix A) which is also consistent with this conjecture. The nontrivial singularity in ρ_Y is related to the nontrivial crossover from the DI to the DP. Then, it is natural to ask what will happen if there is no nontrivial crossover. To answer this question, we study a two-species version of the contact process (CP) with the secondary particles; $X \rightarrow \emptyset$, $X \rightarrow 2X$, $X \rightarrow Y$, and $XY \rightarrow Y$, X , or $2X$ with the crossover parameter w controlling the $X \rightarrow Y$ process and the feedback parameter r controlling the $XY \rightarrow X$. This model belongs to the DP class for any value of w and r , including $w = 0$. Therefore there is no “true” crossover in this model. We found the trivial linear phase boundary ($\Delta_c(w) \sim w$) as expected and also the trivial behavior of ρ_Y with $\alpha = 1$ regardless of the presence of the feedback processes (see Fig. 6). These results are consistent with the mean field results described in the Appendix A.

Up to now, we have been only interested in the emergence of the auxiliary field for a finite crossover parameter w which breaks the mod(2) conservation for the primary particles. One may consider more general cases where the auxiliary field density ρ_Y is finite even at the DI critical point ($w = 0$). First, we studied the crossover behavior to the DP models with a continuous variation of ρ_Y as w increases. We found that $\rho_Y(w) - \rho_Y(0) \sim w^{0.22}$ and the crossover scaling belongs to the CB class [36]. This implies that the vanishing ρ_Y (not just singularity near $w = 0$) is another important ingredient in the CC crossover. Note that $\rho_Y(w)$ seems to behave in the same way as the phase boundary $\Delta_c(w) \sim w^{1/\phi}$ with $1/\phi \simeq 0.22$ for the CB crossover.

Second, there may be a discontinuous drop in ρ_Y in the crossover to the DP with a single absorbing state ($\rho_Y = 0$). This case may be compared to the crossover from the DP with finite ρ_Y (infinitely many absorbing states) to the DP with $\rho_Y = 0$ and similarly from the DI with finite ρ_Y to the DI with $\rho_Y = 0$ [34]. As understood in Ref. [34], this crossover may be characterized by a discontinuous jump in the phase boundary at the DI critical point for the excitatory route or a continuous phase boundary for the inhibitory route. Along the inhibitory route, the CB crossover is observed again (not shown here) and we conclude that the discontinuity in the auxiliary field density does not provide any new crossover scaling [36].

To summarize, we studied three routes of the crossover from the DI to the DP class; symmetry breaking (SB), mod-2 conservation breaking (CB), and channel connecting (CC) routes. These three routes are characterized by three different crossover exponents. The difference between the SB route and the CB route is clear because the symmetry breaking field can be interpreted as the spatial non-local operator affecting the domain wall dy-

namics, while the conservation breaking corresponds to the local operator. The CB route and the CC route share some common features, but the feedback memory effect (or temporal non-locality) makes the CC crossover distinct from the CB crossover. We also found the universal exponent $\alpha = 0.65(2)$ which describes the singularity of the vanishing auxiliary field in the CC route. From the numerical study of the feedback controlling model and its mean field theory, we conjectured that $\alpha = 1 - 1/\phi$.

Acknowledgments

SCP would like to thank for the support of the Korea Institute for Advanced Study (KIAS) where this work was initiated and the support by DFG within SFB 680 *Molecular Basis of Evolutionary Innovations*. Most of computation was carried out using KIAS supercomputers.

APPENDIX A: MEAN FIELD THEORY

This appendix provides the mean field theory for the feedback controlling model introduced in Sec. IV. Here ρ_X and ρ_Y are the densities of X and Y particles, respectively and ρ_Z is the density of sites where both X and Y particles reside. Then one may easily write down the mean field equations as

$$\frac{\dot{\rho}_X}{\rho_X} = 2q - w - 2(1 + q - w)\rho_X - rq \left(\frac{\rho_Z}{\rho_X} - 2\rho_Z \right) \quad (\text{A1})$$

$$\dot{\rho}_Y = w\rho_X - (q + w)\rho_Z, \quad (\text{A2})$$

$$\frac{\dot{\rho}_Z}{\rho_Z} = -1 + (\rho_Y - 2\rho_Z) \left[(1 + q - w) \frac{\rho_X}{\rho_Z} - rq \right], \quad (\text{A3})$$

where $q \equiv 1 - p$. Since $p_c(w = 0) = 1$ in the mean field theory, q is the same as Δ in the text.

In the active phase, the steady state density can be calculated by setting $\dot{\rho}_X = 0$ and so on. The superscript s in the following indicates the steady state density. From Eq. (A2), we get in the active phase

$$\frac{\rho_X^s}{\rho_Z^s} = 1 + \frac{q}{w}. \quad (\text{A4})$$

Hence Eq. (A3) gives the steady state density of ρ_Y^s such that

$$\begin{aligned} \rho_Y^s &= 2\rho_Z^s + \frac{1}{(1 + q - w)\rho_X^s/\rho_Z^s - rq} \\ &= 2\rho_Z^s + \frac{w}{q(1 - wr + q) + w(1 - w)}. \end{aligned} \quad (\text{A5})$$

In the active phase, the (stable) steady state density ρ_Y^s is determined uniquely, so we define the natural density at criticality by taking the limiting process from the active side as $\lim_{q \rightarrow q_c^+} \rho_Y^s(q)$. From Eqs. (A1) and

(A4), the critical point is determined by the equation $-rq + (2q - w)(1 + q/w) = 0$ which reads

$$q_c = \frac{w}{4} \left\{ \sqrt{8 + (1 - r)^2} - (1 - r) \right\}. \quad (\text{A6})$$

For any value of $r(\leq 1)$, $q_c \sim \Delta_c \sim w$ which gives $\phi = 1$. Since $\rho_Z^s = 0$ at criticality, we get $\rho_Y^s \sim w/q_c \sim w^0$ from Eq. (A5), yielding $\alpha = 0$. In low dimensions, q_c is expected to renormalize such that $q_c \sim \Delta_c \sim w^{1/\phi}$, which leads the conjecture $\alpha = 1 - 1/\phi$.

For comparison, we study the two-species version of the contact process with the secondary particles introduced in Sec. IV. The mean field equations are

$$\dot{\rho}_X = (2q - 1)\rho_X - q\rho_X^2 - rq\rho_Z(1 - \rho_X), \quad (\text{A7})$$

$$\dot{\rho}_Y = w\rho_X - (q + w)\rho_Z, \quad (\text{A8})$$

$$\dot{\rho}_Z = -\rho_Z + q(\rho_Y - \rho_Z)(\rho_X - r\rho_Z), \quad (\text{A9})$$

where $q = 1 - p$. Then one may easily show that the critical line and the critical steady-state density of Y particles are given as for small w

$$\begin{aligned} \Delta_c &\simeq \frac{r}{2}w, \\ \rho_Y^s &= \frac{w}{q_c^2 + q_c(1 - r)w} \simeq 4w, \end{aligned} \quad (\text{A10})$$

where $\Delta_c = q_c(w) - 1/2$. As expected, we find the trivial phase boundary and also the trivial value of $\alpha = 1$, which is consistent with the simulation results shown in Fig. 6. Moreover, the renormalization cannot generate a singular behavior in the denominator of Eq. (A10), so α is always expected to be 1 in all dimensions.

-
- [1] H. Hinrichsen, *Adv. Phys.* **49**, 815 (2000); G. Ódor, *Rev. Mod. Phys.* **76**, 663 (2004).
- [2] H. K. Janssen, *Z. Phys. B: Condens. Matter* **42**, 151 (1981).
- [3] P. Grassberger, *Z. Phys. B: Condens. Matter* **47**, 365 (1982).
- [4] G. Grinstein, Z.-W. Lai, D.A. Browne, *Phys. Rev. A* **40**, 4820 (1989).
- [5] I. Jensen, *Phys. Rev. Lett.* **70**, 1465 (1993).
- [6] W. Hwang and H. Park, *Phys. Rev. E* **59**, 4683 (1999).
- [7] M. C. Marques and J. F. F. Mendes, *Eur. Phys. J. B* **12**, 123 (1999).
- [8] H. S. Park and H. Park, *J. Korean Phys. Soc.* **38**, 494 (2001).
- [9] For a review, see M. Henkel and H. Hinrichsen, *J. Phys. A* **37**, R117 (2004).
- [10] J. Kockelkoren and H. Chaté, *Phys. Rev. Lett.* **90**, 125701 (2003).
- [11] J. D. Noh and H. Park, *Phys. Rev. E* **69**, 016122 (2004).
- [12] S.-C. Park and H. Park, *Phys. Rev. Lett.* **94**, 065701 (2005); *Phys. Rev. E* **71**, 016137 (2005).
- [13] H. Hinrichsen, *Physica A* **361**, 457 (2006).
- [14] S.-C. Park and H. Park, *Phys. Rev. E* **73**, 025105(R) (2006).
- [15] P. Grassberger, F. Krause, and T. von der Twer, *J. Phys. A* **17** L105 (1984); P. Grassberger, *ibid.* **22**, L1103 (1989).
- [16] H. Takayasu and A. Yu. Tretyakov, *Phys. Rev. Lett.* **68**, 3060 (1992).
- [17] M. H. Kim and H. Park, *Phys. Rev. Lett.* **73**, 2579 (1994); H. Park, M. H. Kim, and H. Park, *Phys. Rev. E* **52**, 5665 (1995).
- [18] N. Menyhárd, *J. Phys. A* **27**, 6139 (1994); N. Menyhárd and G. Ódor, *ibid.* **29**, 7739 (1996).
- [19] I. Jensen, *Phys. Rev. E* **50**, 3623 (1994).
- [20] W. Hwang, S. Kwon, H. Park, and H. Park, *Phys. Rev. E* **57**, 6438 (1998).
- [21] J. D. Noh, H. Park, and M. den Nijs, *Phys. Rev. E* **59**, 194 (1999).
- [22] O. A. Hammal, H. Chaté, I. Dornic, M. A. Muñoz, *Phys. Rev. Lett.* **94**, 230601 (2005).
- [23] S.-C. Park and H. Park, *Europhys. J. B* **xx** xxxx (2008) (DOI:10.1140/epjb/e2008-00022-4).
- [24] K. Park, H. Hinrichsen, and I.-M. Kim, *Phys. Rev. E* **63**, 065103 (2001).
- [25] H. Park and H. Park, *Physica A* **221**, 97 (1995).
- [26] K.E. Bassler and D.A. Browne, *Phys. Rev. Lett.* **77**, 4094 (1996); *Phys. Rev. E* **55**, 5225 (1997).
- [27] H. Hinrichsen, *Phys. Rev. E* **55**, 219 (1997).
- [28] S. Kwon, W. Hwang, and H. Park, *Phys. Rev. E* **59**, 4949 (1999).
- [29] S. Kwon and H. Park, *Phys. Rev. E* **52**, 5955 (1995).
- [30] J. L. Cardy and U. C. Täuber, *Phys. Rev. Lett.* **77**, 4780 (1996); *J. Stat. Phys.* **90**, 1 (1998).
- [31] N. Inui and A. Yu. Tretyakov, *Phys. Rev. Lett.* **80**, 5148 (1998).
- [32] See, e.g., I.D. Lawrie and S. Sarbach, in *Phase Transitions and Critical Phenomena*, edited by C. Domb and J.L. Lebowitz (Academic Press, London, 1984), Vol. 9.
- [33] G. Ódor and N. Menyhárd, arXiv:0804.3092.
- [34] S.-C. Park and H. Park, *Phys. Rev. E* **76**, 051123 (2007).
- [35] G. Ódor, J. F. F. Mendes, M. A. Santos, and M. C. Marques, *Phys. Rev. E* **58**, 7020 (1998).
- [36] S.-C. Park and H. Park (unpublished).